Synthesis of New Amphiphilic Diblock Copolymers and Their Self-Assembly in Aqueous Solution

Sébastien Garnier[†] and André Laschewsky*[,†,‡]

Universität Potsdam, P.O Box 601553, D-14415 Potsdam, Germany, and Fraunhofer Institute for Applied Polymer Research FhG-IAP, Geiselbergstrasse 69, D-14476 Potsdam-Golm, Germany

Received April 1, 2005; Revised Manuscript Received June 30, 2005

ABSTRACT: Amphiphilic diblock copolymers composed of poly(butyl acrylate) as the hydrophobic block with a low glass transition temperature and of six different hydrophilic blocks (one anionic, one cationic, and four nonionic hydrophilic blocks) are prepared via reversible addition fragmentation chain transfer (RAFT) polymerization. The nonionic hydrophilic blocks comprise in addition to the classical poly(dimethylacrylamide), the thermally sensitive poly(*N*-acryloylpyrrolidine), and a comb-type polymer made of a poly(ethylene glycol acrylate) macromonomer, as well as a new strongly hydrophilic sulfoxide polymer. The "living" character of the polymerizations is supported by very low polydispersity indexes and a good correlation between the molar masses obtained and the theoretically expected ones. Two distinct glass transition temperatures were found by differential scanning calorimetry for the block copolymers, suggesting the immiscibility of the blocks in bulk. The self-assembling properties of the amphiphilic diblock copolymers in aqueous and organic media were studied by nuclear magnetic resonance spectroscopy and dynamic light scattering, as a function of the polarity of the hydrophilic blocks, the ratio of the lengths of the two blocks, and the overall molar mass of the diblock copolymers. Micellelike aggregates with diameters from 25 to 100 nm in water are found, as well as inverse micelles in organic solvents. The length of the hydrophobic block seems to be the main factor governing the size of the aggregates in water. The aggregates are very stable upon dilution and temperature cycles. For large hydrophobic blocks, big structures are observed in addition to small micelles initially after the dispersion in water. As the big aggregates disappear slowly, the micellization process seems thermodynamically favored. If two populations of micelles made from different block copolymers are brought together, "mixed" micelles are formed. The implicit exchange of polymers proves the dynamic character of the micellar systems based on poly(butyl acrylate) as hydrophobic block.

1. Introduction

Amphiphilic block copolymers, which consist of a hydrophobic block that is insoluble in water and a water-soluble hydrophilic block,[1−4] are widely discussed as "macrosurfactants". They have been investigated in numerous application fields such as rheology modifiers,[4] emulsifiers,[5−7] stabilizing agents of latexes,[8−11] demulsifiers,[4] efficiency boosters in microemulsions,[12−15] or flocculants.[5] Amphiphilic block copolymers have also served as solubilizing agents for hydrophobic dyes,[16−19] for liquid crystals,[20] and for metal salts.[21] Moreover, they have been studied as controlled drug delivery systems[22−25] and light harvesting studies.[26] When a block copolymer is dissolved in a solvent that is a thermodynamically good solvent for one block and a nonsolvent for the other one, the polymer chains can reversibly assemble into micellar aggregates, the covalent bond between the blocks preventing macrophase separation.[27] This aggregation process in a selective solvent is analogous to the micellization of low-molar-mass surfactants. However, in comparison to the latter, amphiphilic diblock copolymers have reduced mobility and slower diffusion rates, narrower solubility windows and much lower critical micelle concentrations (cmc).[1] The often kinetically controlled self-aggregation of amphiphilic block copolymers can lead to more than 30 different morphologies.[3] For instance, spherical and hexagonal micelles, rods, lamellae, or vesicles can be formed, depending on the three main forces governing their association process: the stretching of the core-forming block, inter-coronal interactions, and the interfacial energy between the micellar core and the selective solvent.[28] In the simplest case of amphiphilic diblock copolymers, the morphology of the aggregates is controlled by structural factors such as the polarity of each block,[4] the relative lengths of the blocks,[29−33] and the overall molar mass of the polymers.[34] Moreover, the preparation conditions such as the initial polymer concentration[35,36] and the cosolvent used in the dialysis technique[35,37] can influence the morphology of the aggregates formed. External factors, such as temperature[35,38] or the addition of salt,[39] will influence the aggregation behavior, too.

The emergence of methods of controlled free-radical polymerizations in the past decade has simplified the synthesis of tailor-made macrosurfactants, in comparison to the classical methods of living anionic and cationic polymerization. These new methods have also increased the chemical diversity of the useful hydrophilic blocks considerably. Atom transfer radical polymerization (ATRP),[40−45] nitroxyl mediated polymerization (NMP),[46−50] and reversible addition fragmentation chain transfer polymerization (RAFT)[5−7,10,26,33,51−55] are efficient techniques for the synthesis of well-defined amphiphilic diblock copolymers, with controlled molar masses and ratios of the blocks.

Among these options, RAFT polymerization was chosen by us since it can be applied to a wide range of monomers, and it is very tolerant toward experimental

* Corresponding author. Telephone: +493315681327. Fax: +493315683000. E-mail: Laschewsky@iap.fhg.de.
[†] Universität Potsdam.
[‡] Fraunhofer Institute for Applied Polymer Research FhG-IAP.

10.1021/ma0506785 CCC: $30.25
Published on Web 08/13/2005

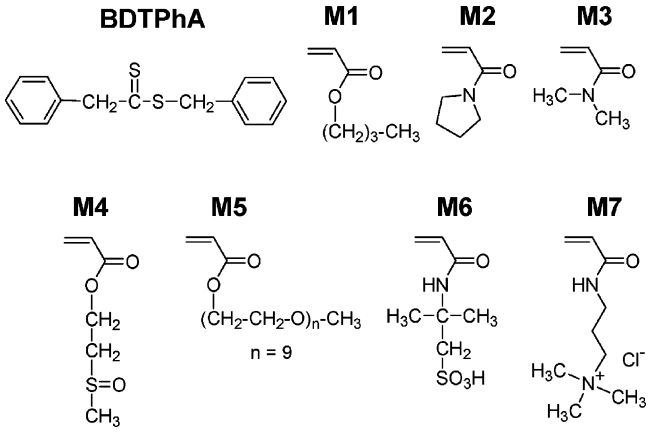

Figure 1. RAFT agent and monomers used.

conditions (temperature, solvent, etc.). Moreover, the RAFT method generally provides very clean polymers. This is very important for studying amphiphilic diblock copolymers, since their behavior can be very sensitive even to small amounts of impurities (such as residual catalysts from ATRP).[54] Furthermore, the RAFT method often allows the degree of functionality of the first block to be conveniently determined by end group determination via the visible absorbance band of the thiocarbonyl group of the RAFT agents.[55] This is most useful for the synthesis of well-defined block copolymers. Still, surprisingly few studies have reported so far on the synthesis of amphiphilic block copolymers by the RAFT technique. The direct preparation of such block copolymers by sequential polymerization of a hydrophobic and a hydrophilic monomer, without any additional chemical modification, is even exceptional [6,7,26,33,53,55] and is mostly confined to acrylic acid as hydrophilic monomer.

In this work, we describe the synthesis of amphiphilic diblock copolymers with various molar masses for both blocks via RAFT polymerization using benzyldithiophenyl acetate **BDTPhA** (Figure 1) as chain transfer agent (CTA). All systems studied are made of the hydrophobic block poly(butyl acrylate) **poly(M1)** which has a low glass transition temperature (T_g), to avoid the formation of "frozen" micelles in water.[3,4] A series of polymers with different hydrophilicities were used as hydrophilic blocks. These are, from the least to the most hydrophilic ones: poly(*N*-acryloyl pyrrolidine) [**poly(M2)**], poly(dimethyl acrylamide) [**poly(M3)**], poly(2-(acryloyloxy ethyl) methyl sulfoxide) [**poly(M4)**], poly(poly(ethylene glycol) methyl ether acrylate) [**poly(M5)**], anionic poly(2-acrylamido-2-methylpropanesulfonic acid) [**poly(M6)**], and cationic poly(3-acrylamidopropyltrimethylammonium chloride) [**poly(M7)**]. The poly(acrylamide)s **poly(M2), poly(M3), poly(M6)**, and **poly(M7)** are classical hydrophilic blocks, which have been widely involved in the study of the self-assembly properties of amphiphilic diblock copolymers.[54,56,57] Moreover, the successful synthesis and blocking of **poly(M3)**[55,58−60] and anionic **poly(M6)**[61−63] by RAFT polymerization have been described in several reports. Among the poly(acrylamide)s synthesized, **poly(M2)** may lead to temperature sensitive aggregation properties, since it exhibits a lower critical solution temperature (LCST) in water.[5,54,64] In addition to the various poly(acrylamide)s, poly(acrylate) **poly(M5)** was used as hydrophilic block. This block is strongly hydrophilic, due to its comb-type structure containing poly(ethylene oxide) (PEO) side chains. Finally, we studied a poly(sulfoxide) as an alternative hydrophilic block, namely **poly(M4)**. This polymer has been hardly described in the past,[65−68] while its synthesis by RAFT and use in amphiphilic block copolymers are unknown. Since the sulfoxide polymer is strongly hydrophilic,[68,69] it is an attractive candidate for the investigation of the self-assembly properties of amphiphilic diblock copolymers. Furthermore, such block copolymers may be of great interest for biomedical and pharmaceutical applications, since **poly(M4)** shows low toxicity.[66,67]

The structural parameters of the amphiphilic systems studied are thus the polarity of the hydrophilic block, the relative molar mass of the blocks, and the overall molar mass of the diblock copolymers. The influence of these structural parameters and of external factors (e.g., the solvent used for the micelle preparation, temperature) on the micellization process of the amphiphilic diblock copolymers was studied in water and in organic solvents.

2. Experimental Section

2.1. Materials. *n*-Butyl acrylate (99+%) (**M1**), dimethyl acrylamide (99+%) (**M3**), poly(ethylene glycol) methyl ether acrylate (M_r = 454) (**M5**), 3-acrylamidopropyltrimethylammonium chloride (75% in water) (**M7**) were purchased from Aldrich. 2-Acrylamido-2-methylpropanesulfonic acid (AMPS) (**M6**) was a gift from Lubrizol France. **M1**, **M3**, and **M5** were purified prior to polymerization by column filtration (aluminum oxide, activated, activity I, basic, 50−200 mesh, Acros Organics) to remove inhibitors and stored at +4 °C in the dark. The aqueous solution of **M7** was extracted thrice with diethyl ether to remove inhibitor 4-methoxyphenol. The syntheses of the monomers *N*-acryloylpyrrolidine[54] (**M2**) and (2-(acryloyloxide ethyl) methyl sulfoxide)[68] (**M4**) and of the RAFT agent benzyl dithiophenylacetate[54] (**BDTPhA**) are described elsewhere. Tetrahydrofuran (99+%) (THF) was dried by distillation from Na/K. Dimethylformamide (DMF), dimethylacetamide (DMA), and *N*-methylpyrrolidone (NMP) used for polymerization were all analytical grade and were passed through basic Al_2O_3 (activated, activity I, basic, 50−200 mesh, Acros Organics) to remove inhibitors. Chloroform-*d* (99.8 atom, D %), deuterium oxide (99.8 atom, D%), d-dimethyl sulfoxide (99.8 atom, D %) and *d*-acetone (99.8 atom, D %) were obtained from Acros Organics. 2,2′-Azobis(isobutyronitrile) (AIBN) was a gift of Wako Pure Chemical Industries. Dialysis tubes "Zellu Trans" (nominal molar mass cut off 3500), and "Zellu Trans" (nominal molar mass cut off 1000), were obtained from Roth. Water used for the preparation of micellar solutions was purified by a Millipore Qplus water purification system (resistance 18 MΩ cm).

2.2. Polymer Synthesis. The conditions for the synthesis of the polymers are summarized in Table 1, and their molecular characterization data are given in Table 2. In a typical procedure for the synthesis of macro RAFT agents **poly(M1)**, butyl acrylate (45.00 g, 351.04 mmol), AIBN (0.0498 g, 0.3033 mmol), **BDTPhA** (0.3858 g, 1.4930 mmol), and THF (45 mL) were placed in a Schlenk tube (see Table 1, entry 5). The samples were deoxygenated by N_2 bubbling for 30 min. The polymerization was performed under vigorous stirring at 66 °C and stopped after 35 min by cooling the mixture quickly to room temperature. Finally, the mixture was freeze-dried in benzene, to remove the solvent and residual monomer. The macro-RAFT agent $\mathbf{(M1)}_{133}$ was obtained as yellow viscous paste, with a conversion of 55%. Theoretically expected molar mass $M_n^{th} = 16.4 \times 10^3$ g·mol^{-1}. SEC (eluent: THF, standard: polystyrene) (see Figure 2): $M_n^{SEC} = 17.0 \times 10^3$ g·mol^{-1}, PDI = 1.21. UV−vis (125.57 g·L^{-1} in butyl acetate): band at λ_{max} = 460 nm, absorbance = 0.289. With ϵ_{BDTPhA} = 39 L·mol^{-1}·cm^{-1}, $M_n^{UV} = 17.0 \times 10^3$ g·mol^{-1} (cf. Table 2, entry 5).

For the synthesis of the diblock copolymers, the specific macro RAFT agent, monomer, initiator and solvent were

Table 1. Polymerization Conditions for the Synthesis of the Macro-RAFT Agents and Diblock Copolymers (66 °C)

entry	polymer	monomer [mmol]	RAFT agent [mmol][a]	AIBN [mmol]	solvent	polym time [min]	convn [%]
1	**(M1)$_{37}$**	175.52	0.74	0.15	22 mL of THF	20	9
2	**(M1)$_{81}$**	351.01	1.47	0.31	45 mL of THF	28	25
3	**(M1)$_{86}$**	351.04	1.49	0.30	45 mL of THF	28	27
4	**(M1)$_{95}$**	175.52	0.74	0.15	22 mL of THF	30	35
5	**(M1)$_{133}$**	351.04	1.49	0.30	45 mL of THF	35	55
6	**(M1)$_{95}$-*b*-(M2)$_{157}$**	6.26	3.56×10^{-2}	1.1×10^{-2}	5 mL of dioxane	90	41
7	**(M1)$_{37}$-*b*-(M3)$_{70}$**	25.24	0.10	1.67×10^{-2}	4 mL of dioxane	30	9
8	**(M1)$_{37}$-*b*-(M3)$_{145}$**	25.24	0.10	1.67×10^{-2}	4 mL of dioxane	60	> 20
9	**(M1)$_{86}$-*b*-(M3)$_{125}$**	10.93	4.50×10^{-2}	7.9×10^{-3}	4 mL of dioxane	60	27
10	**(M1)$_{86}$-*b*-(M3)$_{138}$**	21.94	0.11	1.44×10^{-2}	8 mL of dioxane	90	45
11	**(M1)$_{133}$-*b*-(M3)$_{146}$**	14.27	6.07×10^{-2}	9.4×10^{-3}	6 mL of dioxane	90	33
12	**(M1)$_{37}$-*b*-(M4)$_{59}$**	7.74	5.39×10^{-2}	1.52×10^{-2}	10 mL of DMA	20	29
13	**(M1)$_{37}$-*b*-(M4)$_{106}$**	7.74	5.39×10^{-2}	1.52×10^{-2}	10 mL of DMA	110	74
14	**(M1)$_{95}$-*b*-(M4)$_{52}$**	3.65	2.54×10^{-2}	6.1×10^{-3}	5 mL of DMA	60	26
15	**(M1)$_{95}$-*b*-(M4)$_{190}$**	7.34	2.47×10^{-2}	6.1×10^{-3}	5 mL of DMA	60	37
16	**(M1)$_{133}$-*b*-(M4)$_{53}$**	4.35	2.94×10^{-2}	1.30×10^{-2}	7 mL of DMA	30	22
17	**(M1)$_{133}$-*b*-(M4)$_{93}$**	4.35	2.94×10^{-2}	1.30×10^{-2}	7 mL of DMA	60	62
18	**(M1)$_{133}$-*b*-(M4)$_{106}$**	4.35	2.94×10^{-2}	1.30×10^{-2}	7 mL of DMA	90	75
19	**(M1)$_{81}$-*b*-(M5)$_{95}$**	13.55	9.62×10^{-2}	1.54×10^{-2}	20 mL of THF	180	69
20	**(M1)$_{95}$-*b*-(M5)$_{42}$**	2.19	4.09×10^{-2}	7.3×10^{-3}	5 mL of THF	90	55
21	**(M1)$_{81}$-*b*-(M6)$_{136}$**	22.16	9.80×10^{-2}	1.95×10^{-2}	30 mL of NMP	240	17
22	**(M1)$_{95}$-*b*-(M6)$_{58}$**	4.74	4.22×10^{-2}	9.1×10^{-3}	10 mL of NMP	90	53
23	**(M1)$_{81}$-*b*-(M7)$_{55}$**	2.80	2.36×10^{-2}	3.9×10^{-3}	10 mL of DMF	330	32
24	**(M1)$_{81}$-*b*-(M7)$_{105}$**	4.10	2.39×10^{-2}	8.5×10^{-3}	10 mL of NMP	330	59

[a] For diblock copolymers, amount of macro RAFT agent in mmol, with the assumption 100% functionalization. Conversion determined by gravimetry. THF: tetrahydrofuran. DMA: dimethylacetamide. NMP: *N*-methylpyrrolidone. DMF: dimethylformamide.

Table 2. Characterization of the Macro-RAFT Agents and Diblock Copolymers

entry	polymer	$M_n \times 10^{-3}$ [g/mol][a] SEC	PDI[a] SEC	$M_n \times 10^{-3}$ [g/mol][b] UV	$M_n \times 10^{-3}$ [g/mol][c] microanalysis	$M_n \times 10^{-3}$ [g/mol][d] ^{1}H NMR	theoretical $M_n \times 10^{-3}$ [g/mol][e]
1	**(M1)$_{37}$**	4.8	1.25	4.9			2.8
2	**(M1)$_{81}$**	10.4	1.12				7.7
3	**(M1)$_{86}$**	11.1	1.16	13.2			7.9
4	**(M1)$_{95}$**	12.2	1.15	15.0			10.8
5	**(M1)$_{133}$**	17.0	1.21	17.0			16.5
6	**(M1)$_{95}$-*b*-(M2)$_{157}$**	26.5	1.26		31.9	31.9	21.2
7	**(M1)$_{37}$-*b*-(M3)$_{70}$**	9.1	1.33		11.7	11.7	7.1
8	**(M1)$_{37}$-*b*-(M3)$_{145}$**	18.0	1.18		18.7	19.5	
9	**(M1)$_{86}$-*b*-(M3)$_{125}$**	30.8	1.17		23.9	23.0	17.6
10	**(M1)$_{86}$-*b*-(M3)$_{138}$**	29.4	1.21		24.7	24.7	20.0
11	**(M1)$_{133}$-*b*-(M3)$_{146}$**	31.2	1.20		31.5	30.7	24.7
12	**(M1)$_{37}$-*b*-(M4)$_{59}$**				15.0	14.4	11.6
13	**(M1)$_{37}$-*b*-(M4)$_{106}$**	8.7	1.42		21.6	22.0	22.0
14	**(M1)$_{95}$-*b*-(M4)$_{52}$**				20.6	20.6	18.3
15	**(M1)$_{95}$-*b*-(M4)$_{190}$**	21.1	1.31		40.7	43.0	30.0
16	**(M1)$_{133}$-*b*-(M4)$_{53}$**				26.5	25.0	22.3
17	**(M1)$_{133}$-*b*-(M4)$_{93}$**				32.1	31.7	31.9
18	**(M1)$_{133}$-*b*-(M4)$_{106}$**				34.2	34.2	35.0
19	**(M1)$_{81}$-*b*-(M5)$_{95}$**					53.5	54.5
20	**(M1)$_{95}$-*b*-(M5)$_{42}$**	18.5	1.34			31.3	25.6
21	**(M1)$_{81}$-*b*-(M6)$_{136}$**				38.6	32.1	18.4
22	**(M1)$_{95}$-*b*-(M6)$_{58}$**				24.2	19.1	24.5
23	**(M1)$_{81}$-*b*-(M7)$_{55}$**				21.8		20.9
24	**(M1)$_{81}$-*b*-(M7)$_{105}$**				32.4		38.3

[a] M_n and PDI determined by RI−SEC in THF for macro RAFT agents and by RI−SEC in NMP for diblock copolymers (calibrations by poly(styrene) standards). [b] M_n determined by UV/vis spectroscopy, using the absorption of dithioester end groups at visible band (ϵ_{CTA} in butyl acetate = 39 L·mol^{-1}·cm^{-1}). It is assumed that no dithioester end group is lost and that the blocking efficiency is 100%. [c] Molar ratio x of the blocks determined from N or S elemental analysis. M_n of block copolymers is calculated from x and the molar mass of **poly(M1)**. [d] Molar ratio x of the blocks determined from the ratio of the integrals of NMR peaks of protons of each block. M_n of block copolymers is calculated from x and the molar mass of **poly(M1)**. [e] Theoretical M_n calculated assuming 100% functionalization of the macro RAFT agent.

engaged as listed in Table 1. In a typical procedure, (Table 1, entry 6): monomer *N*-acryloylpyrrolidine **M2** (0.7835 g, 6.2585 mmol), AIBN (0.0018 g, 1.1×10^{-2} mmol), macro-RAFT agent **(M1)**$_{95}$ (0.4340 g, 3.6×10^{-2} mmol) and dioxane (5 mL) were placed in a Schlenk tube. The sample was deoxygenated by three freeze−pump−thaw cycles and polymerized under vigorous stirring at 66 °C for 90 min. Finally, the solution of diblock copolymer **(M1)$_{95}$-*b*-(M2)$_{157}$** in dioxane was dialyzed against water (nominal molar mass cut off 1000), and lyophilized. After lyophilization, a lightly yellow powder was obtained, with a conversion of 41%. Theoretically expected molar mass for the diblock copolymer $M_n^{th} = M_n^{SEC}$ **(M1)**$_{95}$ + M_n^{th} **poly(M2)** = 21.2×10^3 g·mol^{-1}. SEC (eluent: NMP, standard: polystyrene) (see Figure 4A): $M_n^{SEC} = 26.5 \times 10^3$ g·mol^{-1}, PDI = 1.26. Anal. Found: N, 6.78; C, 65.36; H, 9.38. Calculated molar ratio **poly(M2)/poly(M1)** = 1.65. $M_n^{elemental\ analysis} = 31.9 \times 10^3$ g·mol^{-1}. Calculated molar ratio **poly(M2)/poly(M1)** = 1.65 (from integrals of protons h (2.0) and c (6.6)). $M_n^{NMR} = 31.9 \times 10^3$ g·mol^{-1} (cf. Table 2, entry 6). Copolymers **poly(M1-b-M2)** to **poly(M1-b-M6)** were synthesized in homogeneous solution as

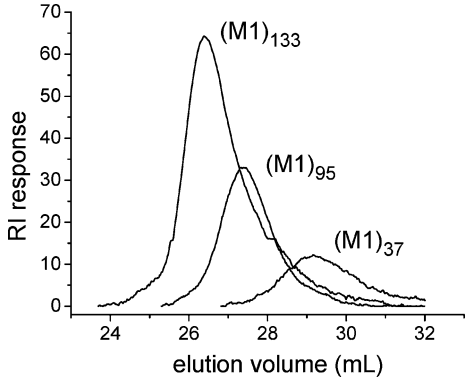

Figure 2. RI detector responses of the SEC chromatograms for macro-RAFT agents **(M1)$_{37}$**, **(M1)$_{95}$**, and **(M1)$_{133}$**. Eluent: tetrahydrofuran. Standard: poly(styrene).

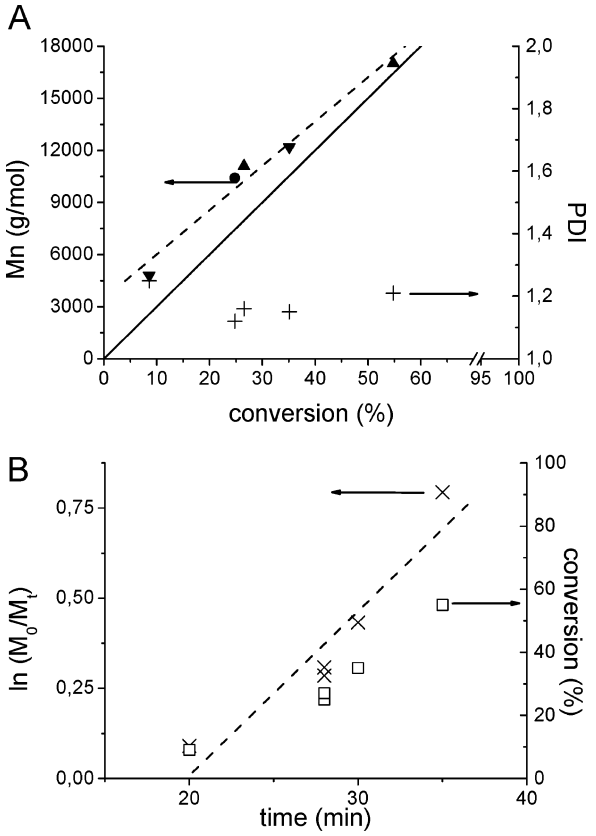

Figure 3. (A): Dependence of M_n (●, ▼, ▲; every symbol indicates a different series of kinetic experiments) and PDI (+) on conversion in the RAFT polymerization of **M1** with benzyldithiophenyl acetate as CTA. Dotted line is the linear fit of M_n vs conversion. Solid line shows the theoretically expected M_n. (B): Conversion vs time (□) and ln(M_0/M_t) vs time (×). Dotted line is the linear fit of ln(M_0/M_t) vs time.

illustrated by the example of **(M1)$_{95}$-*b*-(M2)$_{157}$**, whereas copolymer **poly(M1-b-M7)** was prepared as a dispersion of **M7** in the reaction medium. After the polymerization, the acidic **poly(M6)** blocks were neutralized with stoichiometric amounts of NaOH. In all cases, the diblock copolymers were dialyzed against water (nominal molar mass cut off 1000) and then lyophilized. Conversions were estimated gravimetrically on the basis of copolymer recovered after lyophilization. The absence of residual monomers in the polymers was systematically verified by ^{1}H NMR spectroscopy.

2.3. Methods. ^{1}H (300 MHz) and ^{13}C (75 MHz) NMR spectra were taken with an apparatus Bruker Avance 300 (128 scans for ^{1}H, 10000 scans for ^{13}C). UV−visible spectra were recorded with a UV−vis spectrophotometer Cary-1 (Varian) equipped with temperature controller (Julabo F-10).

Elemental analysis was performed with a model EA 1110 (CHNS−O) from CE Instruments.

Size exclusion chromatography (SEC) in THF was performed at 20 °C using a Waters 515 HPLC isocratic pump equipped with a Waters 2414 Refractive Index detector, a Waters 2487 UV detector and a set of Styragel columns (HR 5, HR 45, HR 3, 500−100 000 Da) from Waters. Eluent: THF (HPLC, from Roth). Flow rate: 1.0 mL·min^{-1}. Calibration was performed with poly(styrene) standards from PSS GmbH (Mainz, Germany). SEC in *N*-methylpyrrolidone was performed at 70 °C using a TSP (Thermo Separation Products from Thermo-Finnigan GmbH, Dreiech, Germany) equipped with a Shodex RI-71 Refractive Index detector, a TSP UV detector. PSS GRAM columns (polyester columns 100 and 1000 Å) from PSS GmbH (Mainz, Germany) were used. Eluent: *N*-methylpyrrolidone (99+ %, Fluka) with 0.05 mol·L^{-1} LiBr (Flow rate: 0.800 mL·min^{-1}). Calibration was performed with poly(styrene) standards from PSS GmbH (Mainz, Germany).

Thermal properties of the polymers were measured with a TGA/SDTA 851 thermal gravimetric analyzer (TGA) (Mettler Toledo) and a DSC 822 differential scanning calorimeter (DSC) (Mettler Toledo) under nitrogen atmosphere. For TGA measurements, 2.0−5.0 mg of the synthesized polymers were scanned at a rate of 20 °C·min^{-1} from 25 to 80 °C, kept at 80 °C for 20 min, and then scanned at a rate of 20 °C·min^{-1} from 80 to 700 °C. The DSC instrument was calibrated by indium and zinc for temperature and enthalpy changes. For analysis by DSC, 2.0−20.0 mg of the samples were placed in an aluminum pan. They were scanned from −100 to +200 °C and subsequently cooled to −100 °C at a rate of 20 °C·min^{-1}, kept for 5 min at −100 °C, and finally reheated to 200 °C with the same rate of 20 °C·min^{-1}. The glass transition temperature (T_g) was evaluated as the midpoint temperature of the characteristic heat capacity change detected in the second heating traces. The recrystallization point (T_r) and the melting point (T_m) were taken as the onset temperature of the exothermic peak and of the endothermic peak respectively, which were observed in the first heating traces.

Dynamic light scattering was performed with a High Performance Particle Sizer (HPPS, from Malvern Instruments) equipped with an He−Ne laser (633 nm) and a thermoelectric Peltier temperature controller (temperature control range: 10−90 °C). The measurements were made at the scattering angle θ = 173 ° ("backscattering detection") at 25 °C. The autocorrelation functions were analyzed with the CONTIN method. The apparent hydrodynamic diameters were calculated according to the Stokes−Einstein equation, $d_{H,app} = kT/3\pi\eta D_{app}$, with D_{app} being the apparent diffusion coefficient and η the viscosity of the solution. Prior to measurement, the polymer solutions were filtered using a Sartorius Ministar-plus 0.45 μm disposable filter and were placed in a polystyrene (water) or glass cuvette (organic solvent). Temperature-dependent DLS experiments were run with a heating program from 25 to 80 °C in steps of 3 °C, equilibrating the samples for 2 min at each step.

The micellar solutions of the block copolymers were prepared as follows. When the hydrophobic block was shorter than the hydrophilic one, polymers were directly dissolved in purified water, with a concentration of 1 g·L^{-1}. When the hydrophobic block was longer than the hydrophilic one, the dialysis method was used. The polymers were dissolved in a cosolvent for 24 h (see Table 3) and dialyzed against purified water for 3 days (nominal molar mass cutoff: 3500). The concentration of the solutions was determined by gravimetry after lyophilisation of 20 mL, and adjusted to 1 g·L^{-1}. For the preparation of inverse micelles, the polymers were directly dissolved in the selective organic solvent with a concentration of 1 g·L^{-1}.

3. Results and Discussion

3.1. Synthesis and Characterization of the Polymers. Synthesis of the Macro RAFT Agents Poly-(M1). The homopolymers **poly(M1)** were synthesized by RAFT polymerization in THF, under the experimen-

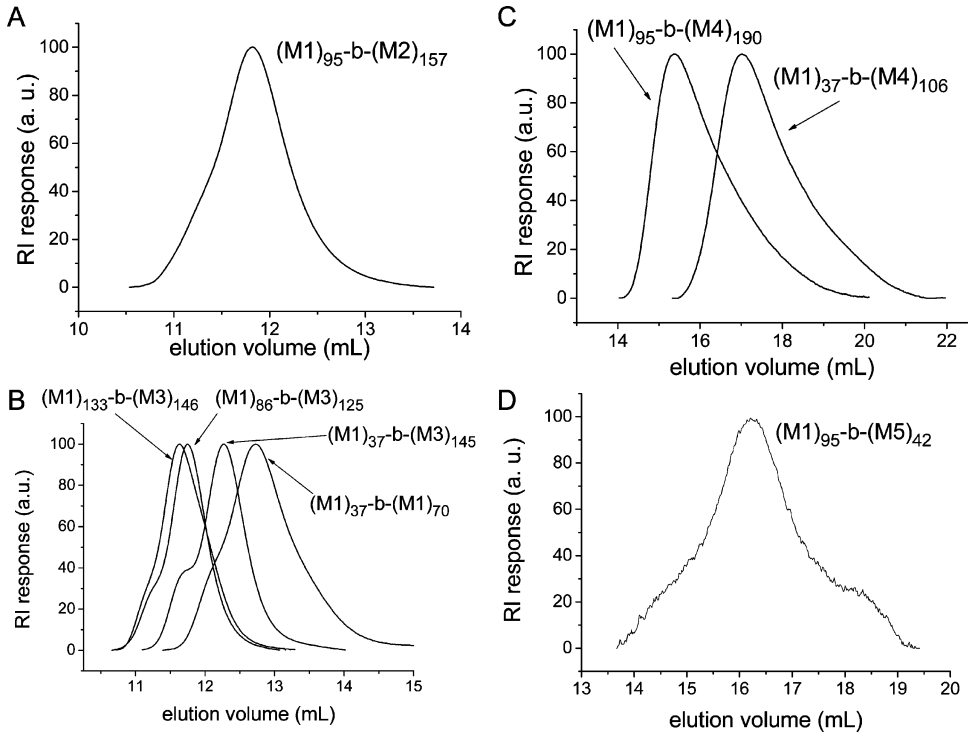

Figure 4. RI detector responses of the SEC chromatograms for diblock copolymers, with **polyM2** (A), **polyM3** (B), **polyM4** (C), and **polyM5** (D) as hydrophilic blocks. Eluent: *N*-methylpyrrolidone. Standard: poly(styrene).

Table 3. Thermal Analysis of Homopolymer $(M1)_{133}$ and Diblock Copolymers by Differential Scanning Calorimetry (DSC)

polymer	T_g [°C][a]	T_g [°C][b]	T_r [°C][c]	T_m [°C][d]
$(M1)_{133}$	−47			
$(M1)_{95}$-*b*-$(M2)_{157}$	−46	142		
$(M1)_{86}$-*b*-$(M3)_{138}$	−46	105		
$(M1)_{37}$-*b*-$(M4)_{106}$	−46	26		
$(M1)_{133}$-*b*-$(M4)_{106}$	−48	30		
$(M1)_{81}$-*b*-$(M5)_{95}$	−63		−53	−18
$(M1)_{95}$-*b*-$(M5)_{42}$	−62		−49	−14
$(M1)_{81}$-*b*-$(M6)_{136}$	−45			
$(M1)_{95}$-*b*-$(M6)_{58}$	−46			
$(M1)_{81}$-*b*-$(M7)_{55}$	−47	50[e]		
$(M1)_{81}$-*b*-$(M7)_{105}$	−49	46[e]		

[a] First glass transition temperature. [b] Second glass transition temperature. [c] Recrystallization temperature. [d] Melting point. [e] T_g determined in the first heating traces.

tal conditions listed in Table 1. Typically, the polymerizations were carried out with a molar ratio CTA/AIBN of 5 and stopped at moderate conversions (<55%), to ensure a good molar mass control and to minimize any loss of dithioester end groups. The rarely used RAFT agent benzyldithiophenyl acetate **BDTPhA**[54] was employed, as benzyl dithioesters and trithioesters are known to be good RAFT agents for acrylic monomers. In particular, the dithiophenyl acetate residue should minimize retardation effects in the polymerization. Whereas the polymerization of poly(acrylate)s via RAFT with the most widely used RAFT agents based on dithiobenzoate generally exhibits an induction period,[70−72] dithiophenyl acetates have been reported to shorten such induction periods considerably.[70,73]

To obtain well-defined block copolymers by RAFT, the order of blocking is crucial.[70,74] However, as the reactivity of acrylates and acrylamides is comparable,[75] the sequence of the blocks can a priori be chosen freely. Often it is preferred to prepare the hydrophilic block first, because it is easier to find a common solvent for a hydrophilic macro-RAFT agent and a hydrophobic monomer,[53] than vice versa. Still, we decided to prepare the hydrophobic **poly(M1)** as initial block in the synthesis of the diblock copolymers, to obtain amphiphilic copolymers with an identical hydrophobic block. This should enable a better comparison of the various systems. Furthermore, **poly(M1)** is more easily characterized by SEC than the various hydrophilic blocks, thus facilitating the determination of the overall molar mass of the block copolymers.

As presented in Figure 2, the SEC traces of the synthesized homopolymers **poly(M1)** show a monomodal, narrow molar mass distribution with polydispersity indexes (M_w/M_n) from 1.12 to 1.25, demonstrating the efficient polymerization control with the RAFT agent chosen for a molar ratio CTA/AIBN of 5. Note that the SEC trace for $(M1)_{133}$ exhibits a small shoulder on the low molar mass side, suggesting a light contamination of the macro-RAFT agent. This could be due to irreversibly terminated end chains, or due to, e.g., minor hydrolysis of the dithioester group.[86] Furthermore, its efficiency in terms of control can be evaluated by a comparison of the experimentally determined molar masses and the theoretically expected molar masses M_n^{th}, given by

$$M_n^{th} = \frac{[\text{monomer}] \times M_{\text{monomer}}}{[\text{CTA}]} \times (\%_{\text{conversion}}) + M_{\text{CTA}} \quad (1)$$

Molar mass values of the macro-CTA **poly(M1)** were determined by SEC according to calibration with poly(styrene), which is an appropriate standard for **poly(M1)** in THF.[76] As shown in Table 2, the M_n values obtained are higher than the theoretical ones, especially at low conversions. A possible explanation for this result could be a hybrid behavior[73] in the initial phase of the polymerization between conventional and living free-radical polymerization. Such a hybrid behavior may be

due to a low chain transfer rate constant in comparison to the propagation rate constant, or may be caused by termination reactions, which lead to fewer active chains. To validate one of these possible explanations, we plotted M_n vs conversion (Figure 3A). It has to be kept in mind that this is no classical polymerization kinetics study, since several polymerizations were performed independently. Nevertheless, the plot of M_n vs conversion shows approximately a linear evolution, demonstrating the excellent reproducibility of the RAFT polymerization of **M1** with **BDTPhA**. Furthermore, we note that the fitted straight line exhibits a positive *y*-intercept. This is known to occur when the rate of polymerization is higher than the rate of addition of growing radicals to the CTA.[77] The molar mass increases very fast at the very beginning of the polymerization, followed by a linear increase up to higher conversions. Further kinetics experiments would be needed to validate this hypothesis of slow radical addition to the CTA, which is however beyond this work. In any case, the polydispersities obtained are low, suggesting that the possible hybrid behavior has a minor effect for the synthesis of the systems studied.

The examination of the plots of $\ln(M_0/M_t)$ and conversion vs time (Figure 3B) reveals an induction period of about 20 min, followed by fast polymerization. Once started, about half of the monomer is consumed within 20 min of ongoing polymerization. The induction period of 20 min when employing **BDTPhA** as RAFT agent is much more shorter than the induction period of about 1 h found in the polymerization of **M1** with cumyl dithiobenzoate or benzyl dithiobenzoate.[72] This observation confirms the expected minimization of the retardation effects in the RAFT polymerization of **M1** when **BDTPhA** is used instead of the classical dithiobenzoates as CTA.[78]

Of particular importance for the synthesis of the second block is the preservation of the active end groups in the macro-RAFT agents. Indeed, inevitable termination reactions can lead to an increasing amount of inactive polymers without reactive end group,[79] or side reactions can result in the degradation of the dithioester group, e.g., by hydrolysis.[55,62,80] Typically, the loss of active end groups increases with ongoing conversion.[81] The yellow color observed for all **P(M1)** samples (λ_{max} = 461 nm) is a good qualitative visual indication of the presence of functional end groups in the polymers. The color originates from a weak absorbance band in the visible range (λ_{max} = 463 nm, ϵ = 45 L mol^{-1} cm^{-1} in hexane, 39 L mol^{-1} cm^{-1} in butyl acetate), due to the forbidden n $\rightarrow$ π^* transition of the $-$C(=S)S- moiety. Moreover, the **BDTPhA** has a strong absorbance band in the UV (λ_{max} = 308 nm, ϵ = 15 000 L mol^{-1}cm^{-1} in hexane), due to the superposed allowed $\pi \rightarrow \pi^*$ transition of the two benzyl moieties. Assuming that the molar extinction coefficient of the dithioester moiety does not change upon incorporation in the polymer and that no important side reactions occur, e.g., chain transfer to the polymer, the visible absorbance band is useful to estimate the extent of functionality of the homopolymers **poly(M1)** used as the macro-RAFT agent. This is done by comparing the molar masses determined by SEC and the molar masses determined by Vis-spectroscopy in butyl acetate. The good agreement of the molar masses determined by SEC and by end group analysis (Table 2) demonstrates that the degree of functionalization of the **poly(M1)** macro-RAFT agents is very high.

Synthesis of the Amphiphilic Diblock Copolymers. The experimental conditions for the RAFT polymerization of the diblock copolymers are listed in Table 1. As for the synthesis of most amphiphilic block copolymers, the appropriate choice of the reaction medium was crucial. The solvents were chosen so that the macro-RAFT agent and the monomer could be dissolved simultaneously. Whereas this was easily feasible for the four nonionic hydrophilic monomers selected, this posed problems in the case of the ionic monomers. Therefore, **M6** was used in its acid form which is soluble in NMP. However, no common solvent could be found for **poly(M1)** and the cationic monomer **M7**. Thus, the latter had to be polymerized as intensively stirred suspension, obtained by adding its concentrated aqueous solution to the solution of the macro-RAFT agents in DMF or NMP. After a short reaction time, the suspension turned into a homogeneous mixture, because of the compatibilizing effect of the amphiphilic copolymers formed with ongoing polymerization. This partially heterogeneous procedure might result in some loss of control of polymerization,[33] although the reaction time in the heterogeneous state was short.

In the case of all uncharged diblock copolymers prepared, both blocks are soluble in NMP. This was demonstrated by monomodal size distribution of DLS data of the polymers in NMP, with a colloidal size between 7 and 9 nm, typical for polymer coils. Accordingly, they could be characterized by SEC in this solvent using poly(styrene) standards. Examples of the chromatograms are shown in Figure 4. Since poly(styrene) standards and the synthesized diblock copolymers have different hydrodynamic radii, the M_n values deduced from SEC are only apparent. Still, the elugrams provide valuable information on the polydispersity of the samples. Typically, the elugrams are monomodal. This and the low polydispersity indexes (Table 2) corroborate the successful and efficient preparation of block copolymers under controlled conditions. For certain samples of **poly(M1-*b*-M3)**, a small high molar mass shoulder is observed (Figure 4B). This could be the result of some bimolecular termination reactions[82] by combination, implying a small amount of triblock copolymer **poly(M1-*b*-M3-*b*-M1)** in the sample. The tiny shoulder at high elution volumes for **(M1)$_{95}$-*b*-(M5)$_{42}$** (Figure 4D) may imply the presence of **poly(M1)** traces in the sample. Concerning the charged block copolymers, no conditions could be found to achieve successful analysis by SEC.

As it is extremely difficult to obtain reliable molar masses for amphiphilic block copolymers from SEC, the overall molar masses of the diblock copolymers were calculated from the molar ratio of the hydrophilic block/hydrophobic block according to ^{1}H NMR and/or elemental analysis. This assumes that the molar mass of the **poly(M1)** block as determined by SEC has not changed (see Table 2). Because of the hygroscopic nature of the polymers, elemental analysis was best evaluated by the ratios of the C/N or C/S contents. Characterization by ^{1}H NMR was best performed in a deuterated good solvent for both blocks (*d*-chloroform for hydrophilic blocks **poly(M2)** to **poly(M5)**, *d*-DMSO for **poly(M6)**). The integrated proton signals of each block with a similar solvation state were compared. The example of **(M1)$_{133}$-*b*-(M4)$_{93}$** in *d*-chloroform is given in Figure 5. The integrals of the peaks of the analogous protons *1*

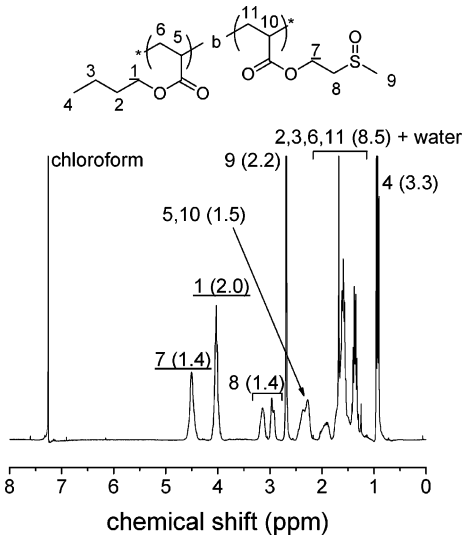

Figure 5. ^{1}H NMR spectrum of diblock copolymer **(M1)$_{133}$-*b*-(M4)$_{93}$** in $CDCl_3$. The numbers indicate the attributed protons, the value between brackets is the integral of the corresponding signal group.

and 7 of both monomer units give a molar ratio block 2/block 1 of 0.70, in excellent agreement with the molar ratio of 0.70 obtained by elemental analysis. As shown in Table 2, the results obtained by ^{1}H NMR and elemental analysis are very consistent for most block copolymers. **Poly(M1-*b*-M7)** was the only system for which no common solvent for both blocks could be found. Thus, no reliable characterization of this block copolymer by ^{1}H NMR was possible.

Note in Table 2 that the experimentally determined molar masses and the theoretically expected values agree well. This corroborates the indications for controlled polymerization of the second, hydrophilic monomers with the macro-RAFT agents **poly(M1)**.

Thermal Analysis of the Polymers. Thermal gravimetric analysis (TGA) showed that all block copolymers undergo thermal degradation above 200 °C. Thus, the thermal characterization of the block copolymers was performed by differential scanning calorimetry (DSC) with subsequent heating/cooling/heating programs from −100 °C to 200 °C. The results are summarized in Table 3. For all polymers except **(M1)$_{133}$** and **poly(M1-*b*-M5)**, a broad endothermic peak was observed in the first heating traces. This signal is attributed to the evaporation of trapped water from the hygroscopic polymers, as it is absent from the second heating cycles on. Homopolymer **(M1)$_{133}$** exhibits a T_g at −47 °C. Block copolymers **poly(M1-*b*-M2)**, **poly(M1-*b*-M3)**, **poly(M1-*b*-M4)**, and **poly(M1-*b*-M7)** exhibit two distinct T_gs. This thermal behavior is exemplified in Figure 6A. The first transition, which occurs in the temperature range from −49 °C to −46 °C, is attributed to the T_g of the hydrophobic block **poly(M1)**. The second one, in the positive temperature range, corresponds to the T_g of the hydrophilic block. Whereas T_g of the block **poly(M1)** stays constant in all heating cycles, the T_g found for the hydrophilic block is increased after the first heating run. This is attributed to the removal of trapped water (see above), which acts as an efficient plasticizer. The occurrence of two distinct T_gs indicates that the two blocks of the three nonionic amphiphilic polymers are immiscible in bulk. This is also true for the cationic block copolymer. In the case of the anionic **poly(M1-*b*-M6)**, however, only one T_g was observed at −46 °C, i.e.,

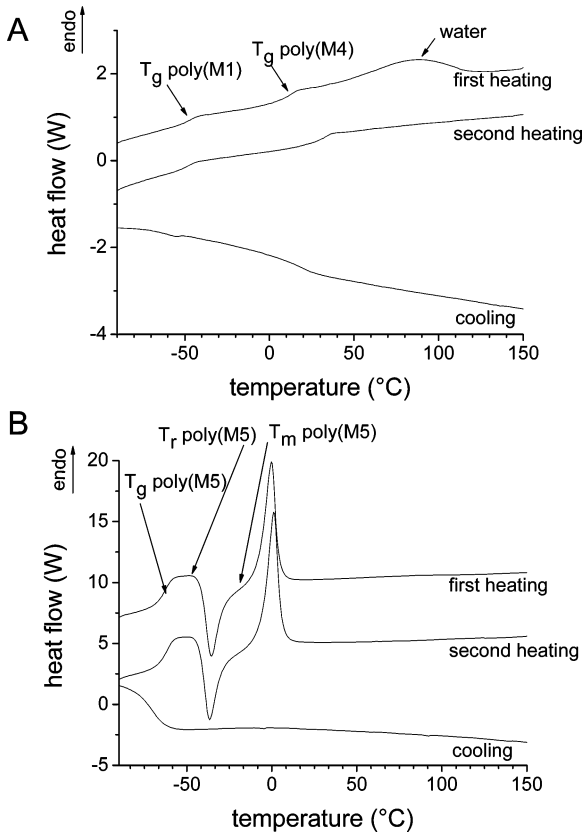

Figure 6. Differential scanning calorimetry (DSC) traces of **(M1)$_{133}$-*b*-(M4)$_{106}$** (A) and **(M1)$_{95}$-*b*-(M5)$_{42}$** (B).

at the T_g of the hydrophobic block **poly(M1)**. Noteworthy, no T_g could be found below 200 °C for the anionic homopolymer **poly(M6)**. Generally, if two polymeric segments are miscible in bulk, this results in an unique glass transition that occurs at an intermediate temperature between the T_gs of the two polymer blocks.[83] Therefore, the occurrence of only one glass transition at the T_g of the **poly(M1)** block strongly suggests that the blocks of **M1** and **M6** are immiscible in bulk, too.

Finally, the thermal analysis of **poly(M1-*b*-M5)** is exemplified by Figure 6B. The DSC trace shows a T_g at −65 °C clearly below the T_g of the hydrophobic block **poly(M1)**, as well as a process at about −50 °C followed by a melting process at about −15 °C. These thermal transitions correspond to the transitions found for the homopolymer **poly(M5)**. The recrystallization and melting processes are characteristic for the short oligo(ethylene oxide) side chains. The glass transition is attributed to the comb-type block **poly(M5)**, too, either due to its poly(acrylate) backbone or due to its short oligo(ethylene oxide) side chains. In any case, the T_g of the hydrophobic block **poly(M1)** is masked. Still, the conservation of the thermal behavior of the homopolymer **poly(M5)** in the block copolymer **poly(M1-*b*-M5)** strongly suggests that these two polymer blocks are immiscible.

In summary, the DSC measurements indicate that the hydrophobic and the hydrophilic blocks of all block copolymers under investigation are incompatible in bulk. Accordingly, microphase separation in solution is expected, and consequently the aggregation of the block copolymers into micelles in a selective solvent.

3.2. Aggregation Behavior of the Diblock Copolymers. The aggregation behavior of the various copolymers in aqueous and organic media was studied

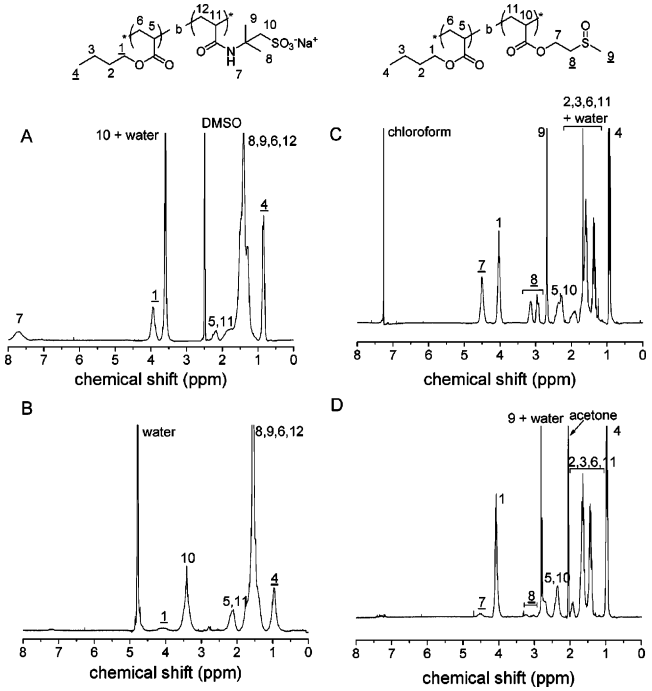

Figure 7. ^{1}H NMR spectra of **(M1)$_{81}$-*b*-(M6)$_{136}$** in *d*-DMSO (A) and D_2O (B) and of **(M1)$_{133}$-*b*-(M4)$_{93}$** in *d*-chloroform (C) and *d*-acetone (D).

preliminarily by ^{1}H NMR spectroscopy and dynamic light scattering (DLS) and correlated to their molecular structure. ^{1}H NMR spectroscopy is a convenient qualitative test for the aggregation of the copolymers in D_2O or in organic deuterated solvents (Figure 7). Parts A and B of Figure 7 present the ^{1}H NMR spectra of the diblock copolymer **(M1)$_{81}$-*b*-(M6)$_{136}$** in *d*-DMSO and D_2O, respectively. The sharp signals of the protons *1* and *4* of the hydrophobic block in *d*-DMSO become remarkably smaller and broadened in D_2O. Accordingly, the corresponding protons are less mobile and less solvated in D_2O. This implies the formation of micellelike aggregates in water, with **poly(M1)** forming the hydrophobic core and **poly(M6)** the hydrophilic corona. Similarly for all nonionic diblock copolymers, the signals of protons *1* and *4* of the hydrophobic block **poly(M1)** are always broadened and show a reduced intensity in D_2O compared to in organic solvents. The analogous situation is encountered in special cases for proton signals of the hydrophilic block in organic solvents. For instance, the signals of the protons *7* and *8* of the hydrophilic block of polymer **(M1)$_{133}$-*b*-(M4)$_{93}$** are well visible and resolved in D_2O and in chloroform (Figure 7C). But they virtually disappear in acetone (Figure 7D) which is a nonsolvent for **poly(M4)**. In the contrary, the signals of the protons *1* and *4* of the hydrophobic block are broadened and weakened in D_2O, whereas they are well resolved and visible in chloroform and acetone. This suggests the formation of inverse micelles in acetone with the hydrophilic block as core and the hydrophobic block as solvated corona. In this respect, the new hydrophilic block **poly(M4)** differs from the behavior of the other nonionic hydrophilic blocks, as the latter are well soluble in acetone and do not form aggregates therein. The particular behavior of the nonionic block **poly(M4)** is attributed to the high dipole moment of the sulfoxide moiety and correlates with its stronger hydrophilicity compared to the poly(acrylamide) blocks used.[68]

Micellization in Water. The preliminary tests by ^{1}H NMR concerning micellization of the copolymers were confirmed by DLS measurements. Homogeneous clear aqueous solutions were obtained by direct dissolution in water only for the diblock copolymers that have strongly hydrophilic blocks, namely **poly(M1)-*b*-(M5)**, **poly(M1)-*b*-(M6)**, and **poly(M1)-*b*-(M7)**, and whose hydrophilic blocks are longer than the hydrophobic ones. In the case of relative long hydrophobic blocks, the stepwise dialysis technique was preferred. This technique allows the continuous and slow exchange of solvents, avoiding or at least minimizing the formation of large aggregates.[4] Depending on the solvent used for the dialysis technique (Table 4), the appearance of the solutions differed from each other. A few systems precipitated, like **(M1)$_{86}$-*b*-(M3)$_{138}$**, **(M1)$_{133}$-*b*-(M3)$_{146}$**, or **(M1)$_{133}$-*b*-(M4)$_{106}$** if chloroform was used to dissolve the copolymer prior to dialysis. This may be explained by the fact that chloroform is not fully miscible with water. The same copolymers did not precipitate when using dimethylacetamide or dioxane as initial solvents. This observation underlines the importance of the choice of the solvent to be used in the dialysis technique, to achieve the preparation of diblock copolymer micelles. Many systems turned slightly cloudy soon after preparation, implying the formation of large aggregates.

DLS analysis of the aqueous solutions indicated the presence of micellar aggregates in the nanometer range (Table 4). Transparent solutions show monomodal particles size distributions with hydrodynamic diameters between 20 and 100 nm. Note that the cationic diblock copolymers **poly(M1-*b*-M7)** form large aggregates with diameters larger than 200 nm, showing a monomodal size distribution. Taking the length of a C−C bond as 0.154 nm,[84] the theoretical maximal value of the diameter of spherical micelles is 57 nm (for maximal chain stretching) for **(M1)$_{81}$-*b*-(M7)$_{105}$**. This simple geometric consideration suggests that the cationic copolymers aggregate into other shapes than spheres. These may be cylindrical micelles or even vesicles, which are favored for ionic block copolymers.[39]

Cloudy solutions presented bimodal or trimodal particles size distributions, i.e., notable amounts of large aggregates (>200 nm) in addition to small micelles. The origin of these large aggregates is not clear yet. They could be intermicellar structures,[33] or colloidal micellelike aggregates stabilized by hydrophilic blocks on the surface.[25] In any case, polymers with longer hydrophobic blocks show a higher tendency to form large aggregates (Table 4). Moreover, the nature of the solvent used for a given hydrophilic block in the dialysis technique seems to influence the amount of large aggregates. For example, the amount of large aggregates of about 300 nm formed by polymer **(M1)$_{95}$-*b*-(M2)$_{157}$** in water increases from 9% to 20% when dioxane is used instead of THF. The same tendency was observed for **(M1)$_{95}$-*b*-(M5)$_{42}$**. However in the case of **(M1)$_{95}$-*b*-(M4)$_{52}$**, the use of THF leads to large aggregates (300 nm) only, whereas the use of dioxane results in the formation of micelles. These results confirm previous reports that the preparation method of micellar solutions of amphiphilic block copolymers, i.e., the history of the sample, is one of the factors controlling the aggregation behavior.[4] Nevertheless, if a given protocol is followed carefully, the preparation of such block copolymer aggregates is fairly reproducible (cf. data in Tables 4 and 5).

Table 4. Dynamic Light Scattering Analysis of 0.1 % Aqueous Solutions of Diblock Copolymers

diblock copolymer	solvent used before dialysis	DLS directly after preparation			DLS 3 months after preparation			δ^e
		D_H [nm][a]	D_H [nm][b]	D_H [nm][c]	D_H [nm][a]	D_H [nm][b]	D_H [nm][c]	
(M1)$_{95}$-*b*-(M2)$_{157}$	dioxane	46 (46)	283 (20)	2400 (33)	51 (93)	303 (6)		0.71
	THF	42 (86)	295 (9)		44 (96)	465 (3)		0.68
(M1)$_{37}$-*b*-(M3)$_{70}$	dioxane	19 (96)	290 (2)		21 (100)			0.65
(M1)$_{37}$-*b*-(M3)$_{145}$	dioxane	36 (90)	290 (9)		36 (100)			0.69
(M1)$_{86}$-*b*-(M3)$_{125}$	dioxane	60 (93)	760 (6)		55 (100)			0.75
(M1)$_{86}$-*b*-(M3)$_{138}$	dioxane	52 (91)	1300 (1)	2200 (6)	54 (100)			0.74
	chloroform	ppt[d]						
(M1)$_{133}$-*b*-(M3)$_{146}$	dioxane	83 (30)	320 (29)	540 (23)	ppt[d]			
	chloroform	ppt[d]			ppt[d]			
	THF	83 (16)	458 (83)					
(M1)$_{37}$-*b*-(M4)$_{59}$	DMA	27 (97)	127 (2)		34 (100)			0.77
(M1)$_{37}$-*b*-(M4)$_{106}$	dioxane	31 (100)			31 (100)			0.69
(M1)$_{95}$-*b*-(M4)$_{52}$	dioxane	35 (16)	260 (13)	2280 (69)	69 (66)	415 (33)		0.85
	THF	300 (71)	2200 (28)		224 (100)			1.08
(M1)$_{95}$-*b*-(M4)$_{190}$	DMA	63 (62)	304 (37)		81 (100)			0.78
	dioxane	62 (5)	320 (26)	530 (21)	69 (32)	516 (67)		0.75
(M1)$_{133}$-*b*-(M4)$_{53}$	DMA	97 (61)	990 (38)		93 (100)			0.87
(M1)$_{133}$-*b*-(M4)$_{93}$	DMA	46 (28)	113 (62)	275 (8)	110 (100)			0.87
(M1)$_{133}$-*b*-(M4)$_{106}$	DMA	99 (55)	307 (37)	503 (7)	143 (100)			0.91
	chloroform	ppt[d]						
(M1)$_{81}$-*b*-(M5)$_{95}$	*f*	52 (100)			52 (100)			0.76
(M1)$_{95}$-*b*-(M5)$_{42}$	dioxane	29 (65)	277 (20)	2200 (13)	31 (87)	250 (12)		0.75
	THF	30 (86)	247 (13)		28 (89)	115 (5)	266 (5)	0.68
(M1)$_{81}$-*b*-(M6)$_{136}$	*f*	43 (100)			43 (100)			0.70
(M1)$_{95}$-*b*-(M6)$_{58}$	DMSO	55 (96)	295 (3)		54 (100)			0.79
(M1)$_{81}$-*b*-(M7)$_{55}$	*f*	224 (100)			261 (100)			1.04
(M1)$_{81}$-*b*-(M7)$_{105}$	*f*	306 (100)			268 (100)			1.17

[a] Hydrodynamic diameter of micelles. 42 (86) means 86 vol % of aggregates with hydrodynamic diameter D_H of 42 nm. [b] Hydrodynamic diameter of second populations of aggregates. [c] Hydrodynamic diameter of third populations of aggregates. [d] Precipitation during dialysis. [e] δ is defined via $D_H \sim N^\delta$, with N overall number-average degree of polymerization of the block copolymer according to ref 29. [f] Polymer directly dissolved in water and not dialyzed.

Table 5. 1:1 Mixtures of Two Micellar Solutions (concentration 1 g L^{-1}) Analyzed by DLS Where the Micellar Solutions before Mixing Were Prepared Like Those in Table 4, but for Different Occasions

diblock copolymers	D_H [nm][a] before mixing	D_H [nm] 3 days after mixing	D_H [nm] 7 months after mixing
(M1)$_{37}$-*b*-(M3)$_{70}$	25 (100)		
+		55 (100)	53 (100)
(M1)$_{86}$-*b*-(M3)$_{138}$	54 (100)		
(M1)$_{81}$-*b*-(M6)$_{136}$	43 (100)		
+		57 (100)	51 (100)
(M1)$_{95}$-*b*-(M6)$_{58}$	54 (100)		
(M1)$_{37}$-*b*-(M3)$_{70}$	25 (100)		
+		192 (100)	181 (100)
(M1)$_{81}$-*b*-(M7)$_{105}$	268 (100)		

diblock copolymers + standard surfactant	D_H [nm] before mixing	D_H [nm] 3 days after mixing	D_H [nm] 4 months after mixing
(M1)$_{86}$-*b*-(M3)$_{138}$	54 (100)		
+		67 (100)	69 (100)
Brij 56	8 (100)		
(M1)$_{133}$-*b*-(M4)$_{53}$	89 (100)		
+		87 (100)	89 (100)
CTAB	3 (100)		

[a] 25 (100) means: 100 vol % of aggregates with hydrodynamic diameter D_H of 25 nm.

As shown in Table 4, the large aggregates almost disappear after 3 months of storage at ambient temperature with no change of the micelle size. This suggests that the systems need long times to equilibrate, despite the low glass transition temperature of the hydrophobic block. This observation is explained by much longer diffusion and exchange rates in solution for amphiphilic block copolymers than for low molar mass surfactants.[4] Since the large aggregates do not grow, but disappear with time, the micellization of the block copolymers seems thermodynamically favored, though kinetically slow.

The thermodynamic state of micellar systems can be characterized by the scaling relation $R \sim N^\delta$ between the characteristic size R of the microstructure (i.e., thickness of a lamellae or a cylinder, diameter of a sphere) and the overall number-average degree of polymerization N of the block copolymers.[29] Table 4 gives the δ values for each system. For most diblock copolymers this value is close to 0.7. This is typical for the "strong segregation limit" regime (SSL), where $R \sim N^{2/3}$ and where the chains have stretched coil configurations. δ values close to unity were obtained for copolymers whose hydrophobic block is longer than the hydrophilic one, and for the cationic systems. This corresponds to the theoretical "super strong segregation limit" regime (SSSL). There, the domains scale as $R \sim N$, and the chain conformation follows the stretched chain statistics.[85] In this case, spheres are disfavored, and block copolymers aggregate to larger morphologies (e.g., cylinders) or bilayers (e.g., vesicles).[35] The thermodynamical regime of strong segregation for the systems studied is in good agreement with the results of the DSC studies, which indicate the incompatibility between the hydrophobic and the hydrophilic blocks.

The micellar hydrodynamic diameters determined by DLS experiments were correlated with the absolute lengths of the hydrophobic block, except for the system **poly(M1-*b*-M7)** which clearly does not form spherical micelles. Note that other systems might form aggregates other than spherical micelles, too, specially for a high ratio hydrophobic block/hydrophilic block. Several reports describe the shape transitions from spheres to cylinders to lamellae with a decrease of the relative length of the hydrophilic block,[30,32,39,86] due to the

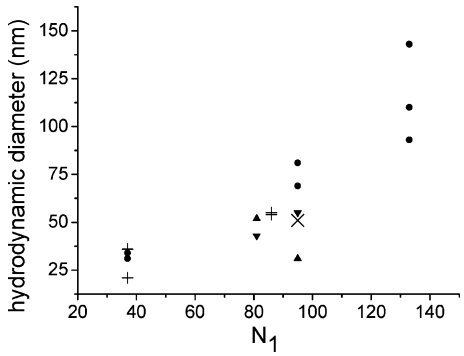

Figure 8. Micellar hydrodynamic diameter determined by DLS vs the number-average of the degree of polymerization (N_1) of the hydrophobic block **poly(M1)**, for **poly(M1)-*b*-poly(M2)** (×), **poly(M1)-*b*-poly(M3)** (+), **poly(M1)-*b*-poly(M4)** (●), **poly(M1)-*b*-poly(M5)** (▲), and **poly(M1)-*b*-poly(M6)** (▼).

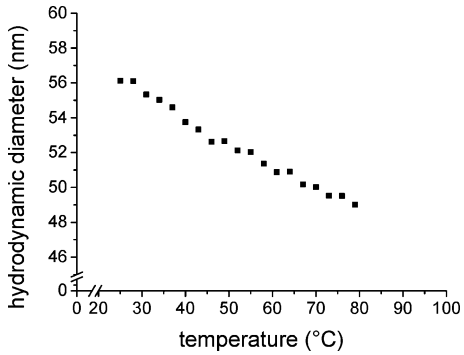

Figure 9. Temperature dependence of micelle size of **$(M1)_{86}$-*b*-$(M3)_{138}$** in water.

increase of the packing parameter and the decrease of the interfacial curvature. This means that polymer **$(M1)_{133}$-*b*-$(M4)_{53}$** for example is a possible candidate to form cylinders or vesicles. The size of 93 nm measured by DLS, much larger than the theoretical maximal diameter of 57 nm of the corresponding sphere, suggests that this polymer forms in water indeed aggregates of nonspherical shape, perhaps vesicles. Consequently, the results obtained by DLS provide an apparent micellar size. As illustrated in Figure 8, the apparent micelle size in water increases with increasing length of the hydrophobic block, in agreement with the literature.[29,31,33,53] In contrast, no general tendency was observed for the influence of the length of the hydrophilic block. Thus, the absolute length of the core-forming block seems to be the most decisive factor controlling the micellar size.

The influence of the length of the corona-forming block on the micellar size seems complex (cf. Table 4). With increasing the length of the hydrophilic block, two opposite behaviors can be expected theoretically. Either the hydrophilic chains become more stretched, resulting in an increase of the micellar size.[87] Alternatively, the larger hydrophilic headgroup requires a larger area of the interface between the hydrophobic core and polar phase, resulting in a decrease of the micellar size.[50] Both scenarios might apply in dependence on the nature of the hydrophilic block. In our case, we observe an increase of the micellar size with increasing the length of the block **poly(M3)**. Copolymer **$(M1)_{37}$-*b*-$(M3)_{70}$** forms aggregates of 21 nm, whereas **$(M1)_{37}$-*b*-$(M3)_{145}$** forms aggregates of 36 nm in diameter. Such a stretching effect is even more pronounced with **poly(M5)** as hydrophilic block. **$(M1)_{81}$-*b*-$(M5)_{95}$** forms larger micelles than **$(M1)_{95}$-*b*-$(M5)_{42}$**, showing that the influence of the hydrophilic block overcompensates even for a somewhat shorter hydrophobic block. This behavior might be due to the macromonomer character of monomer **5**, which results rather in a comb-type polymer than in a linear chain. In the case of the hydrophilic block **poly(M4)**, the results are not conclusive, as increasing molar masses of the block copolymers lead to large aggregates (Table 4) the shapes of which are not clear. Similarly, the influence of the molar mass of the **poly(M6)** block is unclear, since both the hydrophilic and the hydrophobic block increase simultaneously from sample **$(M1)_{81}$-*b*-$(M6)_{136}$** to **$(M1)_{95}$-*b*-$(M6)_{58}$**.

Effect of Dilution. The micellar solutions of diblock copolymers were diluted 10^5 times (i.e., to a concentration of 10^{-5} g L^{-1}) and characterized by DLS after 3 days and after 3 months. No change of aggregate size was observed. As the systems are not frozen (see below), this indicates that the macrosurfactants studied exhibit a very low cmc. This is one of the particularities of amphiphilic diblock copolymers in comparison to standard surfactants.[4] The stability of micellar solutions of diblock copolymers upon dilution can be a great advantage for potential applications.

Temperature Effects on Copolymer Aggregation. Concerning temperature effects, the hydrodynamic diameters of the aggregates of the ionic block copolymers **poly(M1)-*b*-poly(M6)** and **poly(M1)-*b*-poly(M7)** stay virtually the same in the range from 25 to 80 °C. In contrast, we observe a slight decrease of the hydrodynamic diameter of the aggregates with increasing temperature in the same temperature range for the nonionic block copolymers **poly(M1)-*b*-poly(M3)**, **poly(M1)-*b*-poly(M4)**, and **poly(M1)-*b*-poly(M5)**. This is exemplified for **$(M1)_{86}$-*b*-$(M3)_{138}$** in Figure 9, for which the size decreases linearly from 56 to 49 nm between 25 °C and 80 °C. This process is reversible. The effect is attributed to a lower solvation of nonionic hydrophilic blocks in the corona of the micelles at high temperature. According to the reversibility of the thermal changes, the micellar solutions seem to be stable upon temperature changes. In the case of the nonionic block copolymer **poly(M1)-*b*-poly(M2)**, increasing temperature results initially in a gradually reduced hydrodynamic diameter, too. However, above 51 °C, the block copolymer separates out from the solution. This transition is irreversible, as the sedimented block copolymer does not redissolve upon cooling. The particular temperature-sensitive aggregation behavior is not surprising as the homopolymer **poly(M2)** presents a low critical solution temperature (LCST).[54,64] It is interesting to note that the cloud point of the homopolymer in solutions of the same concentration is at 57 °C, i.e., several degrees higher than found for the amphiphilic diblock copolymer. Accordingly, the fixation of the hydrophilic block **poly(M2)** to the hydrophobic block **poly(M1)** reduces its effective hydrophilicity somewhat. This results may seem classical. Indeed, many reports have described the lowering of the thermal transition temperature by increasing statistical incorporation of a hydrophobic monomers in a LCST-polymer.[88–90] However, in the case of amphiphilic block copolymers, diverging behaviors have been reported. For instance, attaching a hydrophobic block to a hydrophilic block exhibiting a LCST transition did not show a significant influence on the transition temperature,[91,92] or occasionally, even an increase of the transition temperature was observed.[54]

Micelle Hybridization. If the core-forming block exhibits a high glass transition temperature, micellar

exchange can become suppressed for block copolymers,[4] so that "frozen" micelles are formed.[31] If dynamic systems are aspired, it is therefore advisable to employ amphiphilic block copolymers which bear a hydrophobic block with a low glass transition temperature, such as **poly(M1)**. Still, in such cases exchange dynamics were reported to be slow.[38,93] To study the micelle exchange dynamics of our systems, the formation of "mixed" micelles was investigated, using the "post-mixing" protocol.[38] Two micellar solutions of two different polymers and of two different aggregate sizes were mixed and stirred for 3 days at 25 °C, before they were characterized by DLS. As shown in Table 5, aggregates with monomodal size distribution were formed after mixing, indicating the formation of mixed micelles. Accordingly, unimer exchange occurred between the two populations of micelles. This proves the mobile character of the micellar systems studied, keeping in mind that the hydrophobic block has a low glass transition temperature (from −50 to −40 °C in bulk). Also, micellar exchange occurs between block copolymer micelles and micelles of low-molecular-weight surfactants. This is exemplified in Table 5 by the nonionic standard surfactant Brij 56 (hexadecaethylene glycolmonodecyl ether, "$C_{10}E_{16}$") and the cationic cetyltrimethylammonium bromide (CTAB). After several months, the mixed systems exhibit the same aggregate sizes as 3 days after mixing. This shows that the thermodynamic equilibrium is reached within a reasonable time (i.e., within 3 days) and that the stable mixed aggregates do not grow into vesicles or bigger morphologies, as it has been often reported for similar hybrid micellar systems.[4]

Formation of Inverse Micelles. ^{1}H NMR spectroscopy of the nonionic block copolymers **poly(M1)-*b*-poly(M4)** suggested the formation of inverse micelles in acetone, with a **poly(M4)** core and a **poly(M1)** corona (cf. Figure 7D). This is corroborated by DLS measurements of **$(M1)_{133}$-*b*-$(M4)_{93}$** in acetone. They indicate the presence of aggregates with a hydrodynamic diameter of 50 nm, exhibiting a monomodal size distribution. Also, inverse micelles are formed by this block copolymer in THF, exhibiting a diameter of 67 nm. The larger aggregate size in THF may be explained by the increasing solvent quality for the core-forming block, resulting in partial swelling. In the case of **$(M1)_{37}$-*b*-$(M4)_{106}$**, the solvophilic block is shortened while the solvophobic block is enlarged. Here, inverse micelles of 94 nm in apparent diameter are formed in acetone. This is larger than the theoretical sphere with fully stretched chains ($D_{th} = 44$ nm), suggesting the formation of nonspherical micelles or larger aggregates.

4. Conclusions

Using the hitherto rarely used chain transfer agent benzyldithiophenyl acetate, the RAFT process allowed the preparation of well-defined amphiphilic diblock copolymers with poly(butyl acrylate) as hydrophobic block. The synthesis of poly(butyl acrylate) exhibited a much shorter induction period than reported for the classical dithiobenzoates as chain transfer agents. Many different hydrophilic blocks with a wide range of hydrophilicities could be employed. This comprised inter alia a strongly hydrophilic polymeric sulfoxide, which does not exhibit the solubility problems encountered for ionic blocks, and which could find biomedical applications. In addition, the RAFT process enabled the polymerization of a hydrophilic macromonomer, to yield a comblike block. For the hydrophobic blocks and all diblock copolymers, low polydispersity indexes as well as the good agreement between the molar masses and the theoretically expected ones showed the controlled character of the polymerizations.

All block copolymers showed microphase separation in bulk according to DSC studies. Also, they self-associated in aqueous medium to yield micellelike aggregates. Their aggregation behavior in water strongly depended on the history of the sample, i.e., the preparation of the micellar solutions. Under optimal preparation conditions, the diblock copolymers formed micelleslike aggregates in the nanometer range in water. Because of the low glass transition temperature of the hydrophobic block poly(butyl acrylate), the micellar systems exhibited a dynamic character, as exemplified by the formation of mixed micelles. Nevertheless, the micelles were very stable upon dilution and no cmc could be measured. The size of the aggregates seems to depend mainly on the length of the hydrophobic block, but to a lesser extent also on the nature of the hydrophilic block. Polymers with high relative ratios hydrophobic block/hydrophilic block formed additionally larger aggregates, which disappeared after a few months, underlining that micellization was thermodynamically favored. The micellar systems are unaffected by a temperature cycle, except for diblock copolymers containing poly(*N*-acryloyl pyrrolidine) as hydrophilic block, which precipitate irreversibly upon heating.

Though the polymer sizes were comparable for the systems studied, the permanently charged hydrophilic block poly(3-acrylamidopropyltrimethylammonium chloride) exhibited a particular aggregation behavior in water, since its block copolymers gave stable large nonspherical morphologies. The poly(sulfoxide) behaved not only as a new strongly hydrophilic block. Moreover, its diblock copolymers formed inverse micelles in organic solvents.

Acknowledgment. We gratefully acknowledge the help by S. Bruzzano and S. Stegmann (Fraunhofer IAP, Golm-Potsdam, Germany) for SEC in THF, by H. Schlaad and M. Gräwert (Max-Planck-Institut für Kolloid- und Grenzflächenforschung, Golm-Potsdam, Germany) for SEC in NMP, and by M. Heydenreich and E. Kleinpeter (Universität Potsdam) for NMR spectroscopy. We are thankful to J. Storsberg (Fraunhofer IAP, Golm-Potsdam, Germany) for the gift of monomer **M2**, and to P. Hennaux (Universität Potsdam) for the gift of monomer **M4**. Financial support by Fonds der Chemischen Industrie is gratefully acknowledged.

Supporting Information Available: Figure S1, giving the ^{1}H NMR spectra of **$(M1)_{133}$** (Tables 1 and 2, entry 5) and **$(M1)_{95}$-*b*-$(M2)_{157}$** (Tables 1 and 2, entry 6) and tables (Tables S1 and S2) of polydispersity values (PDV) for diblock copolymer aggregates according to dynamic light scattering analysis of 0.1% aqueous solutions. This material is available free of charge via the Internet at http://pubs.acs.org.

References and Notes

(1) Laschewsky, A. *Tenside Surf. Det.* **2003**, *40*, 246−249.
(2) Alexandridis, P. *Curr. Opin. Colloid Interface Sci.* **1997**, *2*, 478−489.
(3) Cameron, N. S.; Corbierre, M. K.; Eisenberg, A. *Can. J. Chem.* **1999**, *77*, 1311−1326.
(4) Riess, G. *Prog. Polym. Sci.* **2003**, *28*, 1107−1170.
(5) Storsberg, J.; Laschewsky, A. *SÖFW-J.* **2004**, *130*, 14.

(6) Gaillard, N.; Guyot, A.; Claverie, J. *J. Polym. Sci., Part A: Polym. Chem.* **2003**, *41*, 684−698.
(7) Nikova, A. T.; Gordon, V. D.; Cristobal, G.; Ruela Talingting, M.; Bell, D. C.; Evans, C.; Joanicot, M.; Zasadzinski, J. A.; Weitz, D. A. *Macromolecules* **2004**, *37*, 2215−2218.
(8) Riess, G. *Colloids Surf. A* **1999**, *153*, 99−110.
(9) Tauer, K.; Zimmermann, A.; Schlaad, H. *Macromol. Chem. Phys.* **2002**, *203*, 319−327.
(10) Save, M.; Manguian, M.; Chassenieux, C.; Charleux, B. Macromolecules **2004**, *38*, 280−289.
(11) Riess, G.; Labbe, C. *Macromol. Rapid Commun.* **2004**, *25*, 401−435.
(12) Jakobs, B.; Sottmann, T.; Strey, R. *Langmuir* **1999**, *15*, 6707−6711.
(13) Endo, H.; Allgaier, J.; Mihailescu, M.; Monkenbusch, M.; Gompper, G.; Richter, D.; Jakobs, B.; Sottmann, T.; Strey, R. *Appl. Phys. A: Mater. Sci. Process.* **2002**, *74*, 392−395.
(14) Byelov, D.; Frielinghaus, H.; Allgaier, J.; Gompper, G.; Richter, D. *Physica B* **2004**, *350*, 931−933.
(15) Frielinghaus, H.; Byelov, D.; Allgaier, J.; Gompper, G.; Richter, D. *Physica B* **2004**, *350*, 186−192.
(16) Stepanek, M.; Krijtova, K.; Prochazka, K.; Teng, Y.; Webber, S. E.; Munk, P. *Acta Polym.* **1998**, *49*, 96−102.
(17) Kim, J.-H.; Emoto, K.; Iijima, M.; Nagasaki, Y.; Aoyagi, T.; Okano, T.; Sakurai, Y.; Kataoka, K. *Polym. Adv. Technol.* **1999**, *10*, 647−654.
(18) Chen, X. L.; Jenekhe, S. A. *Langmuir* **1999**, *15*, 8007−8017.
(19) Choucair, A.; Eisenberg, A. *J. Am. Chem. Soc.* **2003**, *125*, 11993−12000.
(20) Fundin, J.; Castelleto, V.; Yang, Z.; Hamley, I. W.; Waigh, T. A.; Price, C. *J. Macromol. Sci., Part B: Phys.* **2004**, *B43*, 893−912.
(21) Antonietti, M.; Förster, S.; Hartmann, J.; Oestreich, S. *Macromolecules* **1996**, *29*, 3800−3806.
(22) Kakizawa, Y.; Kataoka, K. *Adv. Drug Deliv. Rev.* **2002**, *54*, 203−222.
(23) Kabanov, A. V.; Batrakova, E. V.; Alakhov, V. Y. *J. Controlled Release* **2002**, *82*, 189−212.
(24) Bertin, P. A.; Watson, K. J.; Nguyen, S. T. *Macromolecules* **2004**, *37*, 8364−8372.
(25) Park, E. K.; Lee, S. B.; Lee, Y. M. *Biomaterials* **2005**, *26*, 1053−1061.
(26) Chen, M.; Ghiggino, K. P.; Mau, A. W. H.; Rizzardo, E.; Sasse, W. H. F.; Thang, S. H.; Wilson, G. J. *Macromolecules* **2004**, *37*, 5479−5481.
(27) Klok, H.-A.; Lecommandoux, S. *Adv. Mater.* **2001**, *13*, 1217−1229.
(28) Halperin, A.; Tirrell, M.; Lodge, T. P. *Adv. Polym. Sci.* **1992**, *100*, 31−71.
(29) Förster, S.; Zisenis, M.; Wenz, E.; Antonietti, M. *J. Chem. Phys.* **1996**, *104*, 9956−9970.
(30) Zheng, Y.; Won, Y.-Y.; Bates, F. S.; Davis, H. T.; Scriven, L. E.; Talmon, Y. *J. Phys. Chem. B* **1999**, *103*, 10331−10334.
(31) Jain, S.; Bates, F. S. *Macromolecules* **2004**, *37*, 1511−1523.
(32) Lim Soo, P.; Eisenberg, A. *J. Polym. Sci., Part B: Polym. Phys.* **2004**, *42*, 923−938.
(33) Stenzel, M. H.; Barner-Kowollik, C.; Davis, P.; Dalton, H. M. *Macromol. Biosci.* **2004**, *4*, 445−453.
(34) Kaya, H.; Willmer, L.; Allgaier, J.; Stellbrink, J.; Richter, D. *Appl. Phys. A: Mater. Sci. Process.* **2002**, *74*, 499−501.
(35) Yang, Z.; Yuan, J.; Cheng, S. *Eur. Polym. J.* **2005**, *41*, 267−274.
(36) Förster, S.; Antonietti, M. *Adv. Mater.* **1998**, *10*, 195−217.
(37) Zhang, W.; Shi, L.; An, Y.; Gao, L.; Wu, K.; Ma, R. *Macromolecules* **2004**, *37*, 2551−2555.
(38) Won, Y.-Y.; Davis, H. T.; Bates, F. S. *Macromolecules* **2003**, *36*, 953−955.
(39) Förster, S. *Ber. Bunsen-Ges. Phys. Chem.* **1997**, *101*, 1671−1678.
(40) Hussain, H.; Busse, K.; Kressler, J. *Macromol. Chem. Phys.* **2003**, *204*, 936−946.
(41) Sidorov, S. N.; Bronstein, L. M A.; Valetsky, P. M.; Lim Soo, P.; Maysinger, D.; Eisenberg, A. *Langmuir* **2004**, *20*, 3543−3550.
(42) Dai, S.; Ravi, P.; Leong, C. Y.; Tam, K. C.; Gan, L. H. *Langmuir* **2004**, 1597−1604.
(43) Weaver, J. V. M.; Bannister, I.; Robinson, K. L.; Bories-Azeau, X.; Armes, S. P.; Smallridge, M.; McKenna, P. *Macromolecules* **2004**, *37*, 2395−2403.
(44) Ravi, P.; Sin, S. L.; Gan, L. H.; Tam, K. C.; Xia, X. L.; Hu, X. *Polymer* **2005**, *46*, 137−146.
(45) Wang, G.; Tong, X.; Zhao, Y. *Macromolecules* **2004**, *37*, 8911−8917.
(46) Beyou, E.; Humbert, J.; Chaumont, P. *e-Polym.* **2003**, *20*, 1−9.
(47) Lefay, C.; Belleney, J.; Charleux, B.; Guerret, O.; Magnet, S. *Macromol. Rapid Commun.* **2004**, *25*, 1215−1220.
(48) Laruelle, G.; Francois, J.; Billon, L. *Macromol. Rapid Commun.* **2004**, *25*, 1839−1844.
(49) Lacroix-Desmazes, P.; André, P.; Desimone, J. M.; Ruzette, A.-V.; Boutevin, B. *J. Polym. Sci., Part A: Polym. Chem.* **2004**, *42*, 3537−3552.
(50) Matsuoka, H.; Maeda, S.; Kaewsaiha, P.; Matsumoto, K. *Langmuir* **2004**, *20*, 7412−7421.
(51) Pai, T. S. C.; Barner-Kowollik, C.; Davis, T. P.; Stenzel, M. H. *Polymer* **2004**, *45*, 4383−4389.
(52) Nuopponen, M.; Ojala, J.; Tenhu, H. *Polymer* **2004**, *45*, 3643−3650.
(53) Yusa, S.-i.; Fukuda, K.; Yamamoto, T.; Ishihara, K.; Morishima, Y. *Biomacromolecules* **2005**, *6*, 663−670.
(54) Mertoglu, M.; Garnier, S.; Laschewsky, A.; Skrabania, K.; Storsberg, J. *Polymer*, **2005**, *46*, 7726−7740.
(55) Mertoglu, M.; Laschewsky, A.; Skrabania, K.; Wieland, C. *Macromolecules*, **2005**, *38*, 3601.
(56) Fischer, A.; Brembilla, A.; Lochin, P. *Polymer* **2001**, *42*, 1441−1448.
(57) Nowakowska, M.; Szczubialka, K.; Grebosz, M. *J. Colloid Interface Sci.* **2003**, *265*, 214−219.
(58) Rizzardo, E.; Chiefari, J.; Chong, B. Y. K.; Ercole, F.; Krstina, J.; Jeffery, J.; Le, T. P. T.; Mayadunne, R. T. A.; Meijs, G. F.; Moad, C. L.; Moad, G.; Thang, S. H. *Macromol. Symp.* **1999**, *143*, 291−307.
(59) Thomas, D. B.; Convertine, A. J.; Myrick, L. J.; Scales, C. W.; Smith, A. E.; Lowe, A. B.; Vasilieva, Y. A.; Ayres, N.; McCormick, C. L. *Macromolecules* **2004**, *37*, 8941−8950.
(60) Relogio, P.; Charreyre, M.-T.; Farinha, J. P. S.; Martinho, J. M. G.; Pichot, C. *Polymer* **2004**, *45*, 8639−8649.
(61) Sumerlin, B. S.; Lowe, A. B.; Thomas, D. B.; McCormick, C. L. *Macromolecules* **2003**, *36*, 5982−5987.
(62) Thomas, D. B.; Convertine, A. J.; Hester, R. D.; Lowe, A. B.; McCormick, C. L. *Macromolecules*, **2004**, *37*, 1735−1741.
(63) Yusa, S.-i.; Shimada, Y.; Mitsukami, Y.; Yamamoto, T.; Morishima, Y. *Macromolecules* **2004**, *37*, 7507−7513.
(64) Ito, S.; Hirasa, O.; Yamauchi, A. *Kobunshi Ronbunshu* **1989**, *46*, 427−435.
(65) Ritschel, W. A. *Angew. Chem.* **1969**, *81*, 757.
(66) Hofmann, V.; Ringsdorf, H.; Muacevic, G. *Makromol. Chem.* **1975**, *176*, 1929−1943.
(67) Hofmann, V.; Ringsdorf, H. *Makromol. Chem.* **1980**, *181*, 351−366.
(68) Hennaux, P.; Laschewsky, A. *Colloid Polym. Sci.* **2003**, *281*, 807−814.
(69) Hennaux, P.; Laschewsky, A. *Colloid Polym. Sci.* **2001**, *279*, 1149−1159.
(70) Barner-Kowollik, C.; Davis, T. P.; Heuts, J. P. A.; Stenzel, M. H.; Vana, P.; Whittaker, M. *J. Polym. Sci., Part A: Polym. Chem.* **2003**, *41*, 365−375.
(71) Duréault, A.; Taton, D.; Destarac, M.; Leising, F.; Gnanou, Y. *Macromolecules* **2004**, *37*, 5513−5519.
(72) Moad, G.; Chiefari, J.; Chong, Y. K.; Krstina, J.; Mayadunne, R. T. A.; Postma, A.; Rizzardo, E.; Thang, S. H. *Polym. Int.* **2000**, *49*, 993−1001.
(73) Szablan, Z.; Ah Toy, A.; Davis, T. P.; Hao, X.; Stenzel, M. H.; Barner-Kowollik, C. *J. Polym. Sci., Part A: Polym. Chem.* **2004**, *42*, 2432−2443.
(74) Chong, Y. K.; Le, T. P. T.; Moad, G.; Rizzardo, E.; Thang, S. H. *Macromolecules* **1999**, *32*, 2071−2074.
(75) Neugebauer, D.; Matyjaszewski, K. *Macromolecules* **2003**, *36*, 2598−2603.
(76) (a) Schmitt, B. Ph.D. Thesis, Universität Mainz, Germany, 1999. (b) Müller, A. H. E. Personal communication.
(77) Vasilieva, Y. A.; Thomas, D. B.; Scales, C. W.; McCormick, C. L. *Macromolecules* **2004**, *37*, 2728−2737.
(78) Coote, M. L. *Macromolecules* **2004**, *37*, 5023−5031.
(79) Fischer, H. *Chem. Rev.* **2001**, *101*, 3581−3588.
(80) Thomas, D. B.; Sumerlin, B. S.; Lowe, A. B.; McCormick, C. L. *Macromolecules* **2003**, *36*, 1436−1443.
(81) Baussard, J. **2004**, Ph.D. Thesis, Université Catholique de Louvain, Louvain-La-Neuve, Belgium.
(82) Zhu, J.; Zhou, D.; Zhu, X.; Chen, G. *J. Polym. Sci., Part A: Polym. Chem.* **2004**, *42*, 2558−2565.
(83) Yang, J.; Jia, L.; Yin, L.; Yu, J.; Shi, Z.; Fang, Q.; Cao, A. *Macromol. Biosci.* **2004**, *4*, 1092−1104.
(84) Triftaridou, A. I.; Vamvakaki, M.; Patrickios, C. S. *Polymer* **2002**, *43*, 2921−2926.

(85) Nyrkova, I. A.; Khokhlov, A. R.; Doi, M. *Macromolecules* **1993**, *26*, 3601−3610.
(86) Donovan, M. S.; Lowe, A. B.; Sanford, T. A.; McCormick, C. L. *J. Polym. Sci., Part A: Polym. Chem.* **2003**, *41*, 1262−1281.
(87) Pillay Narrainen, A.; Pascual, S.; Haddleton, D. M. *J. Polym. Sci., Part A: Polym. Chem.* **2002**, *40*, 439−450.
(88) Sugiyama, K.; Mitsuno, S.; Yasufuku, Y.; Shiraishi, K. *Chem. Lett.* **1997**, *26*, 219−220.
(89) Laschewsky, A.; Rekaï, E. D.; Wischerhoff, E. *Macromol. Chem. Phys.*, **2001**, *202*, 276−286.
(90) Chee, C. K.; Rimmer, S.; Shaw, D. A.; Soutar, I.; Swanson, L. *Macromolecules* **2001**, *34*, 7544−7549.
(91) Hales, M.; Barner-Kowollik, C.; Davis, T. P.; Stenzel, M. H. *Langmuir* **2004**, *20*, 10809−10817.
(92) Chen, X.; Ding, X.; Zheng, Z.; Peng, Y. *Colloid Polym. Sci.* **2005**, *283*, 452−455.
(93) Creutz, S.; van Stam, J.; De Schryver, F. C.; Jérôme, R. *Macromolecules* **1998**, *31*, 681−689.

MA0506785